Since January 2020 Elsevier has created a COVID-19 resource centre with free information in English and Mandarin on the novel coronavirus COVID-19. The COVID-19 resource centre is hosted on Elsevier Connect, the company's public news and information website.

Virology 537 (2019) 226–236

Contents lists available at ScienceDirect

Virology

journal homepage: www.elsevier.com/locate/virology

Generating and evaluating type I interferon receptor-deficient and feline TMPRSS2-expressing cells for propagating serotype I feline infectious peritonitis virus

Robert C. Mettelman[a], Amornrat O'Brien[a], Gary R. Whittaker[b], Susan C. Baker[a,*]

[a] Department of Microbiology and Immunology, Loyola University Chicago, Stritch School of Medicine, Maywood, IL, United States
[b] Department of Microbiology and Immunology, College of Veterinary Medicine, Cornell University, Ithaca, NY, United States

ARTICLE INFO

Keywords:
Feline coronavirus
FIPV
Crispr/Cas gene editing
IFNαR-deficient cells
Interferon signaling-deficient cells
TMPRSS2-expressing cells
Fcwf-4 CU cells
AK-D cells

ABSTRACT

Feline coronavirus infection can progress to a fatal infectious peritonitis, which is a widespread feline disease without an effective vaccine. Generating feline cells with reduced ability to respond to interferon (IFN) is an essential step facilitating isolation of new candidate vaccine strains. Here, we describe the use of Crispr/Cas technology to disrupt type I IFN signaling in two feline cell lines, AK-D and Fcwf-4 CU, and evaluate the replication kinetics of a serotype I feline infectious peritonitis virus (FIPV) within these cells. We report that polyclonal cell populations and a clonal isolate, termed Fcwf-4 IRN, exhibited significantly diminished IFN-responsiveness and allowed FIPV replication kinetics comparable to parental cells. Furthermore, we demonstrate that replication of FIPV is enhanced by ectopic expression of a host serine protease, TMPRSS2, in these cells. We discuss the potential of these cells for isolating new clinical strains and for propagating candidate vaccine strains of FIPV.

1. Introduction

Feline coronaviruses (FCoVs) are a group of alphacoronaviruses that infect cats and can cause a highly lethal disease known as feline infectious peritonitis (FIP) (Pedersen, 2009). FCoVs are widespread with upwards of 90% of certain domestic feline populations exhibiting seropositivity for these viruses (Addie et al., 2003; Addie and Jarrett, 1992; Hohdatsu et al., 1992; Pedersen, 2009). Despite the severity of this disease and the endemic nature of FCoVs, treatment options are limited. There are no currently approved therapeutics to treat FIP; however, reports of direct inhibition of virus growth and reversal of disease progression in individual cats using small molecule viral inhibitors have been promising (Kim et al., 2016, 2015; 2013, 2012; Pedersen et al., 2019, 2018; St. John et al., 2015). Although these studies demonstrate that treatment of FIP is possible, therapeutic interventions face significant challenges in overcoming the high number of naturally occurring infections. Widespread immunization against FCoV would be the most efficient method to alleviate the burden of disease and reduce the overall density of endemic virus. To date, however, vaccination efficacy has been limited (Pedersen, 2014a).

FCoVs are grouped into two bio- or pathotypes, typically referred to as feline enteric coronavirus (FECV) and feline infectious peritonitis virus (FIPV), based on associated disease progression, tissue tropism and several genetic markers [reviewed in (Kipar and Meli, 2014; Pedersen, 2009)]. Infection by the endemic biotype, FECV, is mild and leads to subclinical, persistent infection in kittens (Addie, 2011; Addie et al., 2003; Merck Veterinary Manual, 2015). However, a subset of FECV infections (3–5%) result in lethal FIP, likely caused when a mutant, highly pathogenic biotype, termed FIPV, arises during replication (Pedersen, 2009; Vennema et al., 1998). FCoVs are further defined by two serotypes based on antigenicity of the viral spike protein (Hohdatsu et al., 1991; Pedersen et al., 1984), although an updated categorization model has recently been proposed (Whittaker et al., 2018). Serotype I FCoVs account for the bulk (80–90%) of naturally occurring infections in domestic cats, while serotype II viruses are responsible for 10–20% of infections in endemic regions [reviewed in (Kipar and Meli, 2014; Pedersen, 2014b)]. Immunization against serotype I FIPV is likely the most effective vaccination strategy to protect against FIP as targeting this highly prevalent serotype would elicit broad herd immunity (Pedersen, 2009); however, implementing an effective serotype I FIPV vaccine has been largely unsuccessful.

One consideration for serotype I FIPV vaccine design is the strength of the innate immune response to immunization. Strong innate responses, typified by high levels of type I interferon (IFN), generally

* Corresponding author.
E-mail address: sbaker1@luc.edu (S.C. Baker).

https://doi.org/10.1016/j.virol.2019.08.030
Received 24 May 2019; Received in revised form 29 August 2019; Accepted 29 August 2019
Available online 30 August 2019

result in robust adaptive responses and development of immune memory (Hoebe et al., 2004; Siegrist, 2013). Coronaviruses (CoVs) including FCoV, however, delay or subvert innate signaling using a number of virus-encoded type I IFN antagonists (Dedeurwaerder et al., 2014; Deng et al., 2017; Kindler et al., 2017; Rose and Weiss, 2009; Totura and Baric, 2012) that limit appropriate inflammatory responses (Channappanavar et al., 2016). In the case of FIPV, infection of monocytes triggers unregulated inflammation and immune-mediated pathology. The adaptive responses, including cytotoxic T cell and humoral B cell stimulation and recruitment are generally weak and do not result in immunologic memory (Tang et al., 2011). As a further complication, antibodies produced against the spike and envelope proteins of FIPV have been shown to mediate antibody-dependent enhancement of disease (Corapi et al., 1992; Olsen et al., 1992), challenging the traditional approaches to surface-antigen vaccine design. Several groups have demonstrated that strong cytotoxic T cell responses during FIPV infection are associated with positive disease outcomes (de Groot-Mijnes et al., 2004; Pedersen, 2014b; Satoh et al., 2011). Importantly, type I IFN signaling has been shown to enhance cytotoxic T cell responses [reviewed in (Meager, 2006; Tough, 2012)] as well as promote memory T cell development [reviewed in (Huber and David Farrar, 2011)]. Thus, a live-attenuated serotype I FIPV strain that stimulates an early type I IFN response may lead to development of long-lasting T cell memory and elicit protection.

Targeted elimination of virus-encoded type I IFN antagonists, resulting in a virus with a “hyper interferon sensitive” (HIS) phenotype, has been a successful method for generating live-attenuated CoV vaccines (Deng et al., 2019, 2017; Kindler et al., 2017; Menachery et al., 2018). In these studies, highly-permissive cells lacking the type I IFN receptor (IFNαR) were critical. Due to the lack of IFN signaling, these IFNαR$^{-/-}$ cells allowed recovery, propagation and characterization of HIS viruses produced by reverse genetics without negative selective pressure or induction of suppressive mutations in the viral genome. We hypothesize that feline cell lines that are i) highly permissive to serotype I FCoV and ii) deficient in IFNαR signaling would allow for the development and investigation of IFN antagonist-deficient FIPV viruses and could be employed in future studies to recover HIS vaccine candidate strains using reverse genetics. However, to our knowledge, a feline IFNαR-deficient cell line permissive to serotype I FIPV was not currently available.

In this study, we sought to eliminate IFN-responsiveness in two serotype I FCoV-permissive cell lines: AK-D, immortalized cells derived from feline lung tissue, and Fcwf-4 Cornell University (CU) (O'Brien et al., 2018), a feline macrophage-like cell line. To this end, we employed the Crispr/Cas gene editing system to disrupt domain 2 of the type I IFN receptor (IFNαR2) in both AK-D and Fcwf-4 CU cell lines. We demonstrate the successful disruption of IFN-responsiveness in both cell populations as well as the isolation of a clonal cell line derived from the IFNαR-null Fcwf-4 CU population. The replication kinetics of serotype I FIPV Black were evaluated in each cell type and we show that the Crispr/Cas-modified cells remain permissive to virus infection. Lastly, we sought to enhance replication of serotype I FCoVs in one of these cell lines to aid in the recovery and growth of serotype I FIPV strains. To this end, we expressed a host transmembrane serine protease, TMPRSS2, and demonstrate enhanced replication of FIPV Black. Together, our data describe the successful generation and characterization of three feline cell lines deficient in IFN signaling, one of which is capable of enhanced FIPV replication through expression of a host protease. We predict that these cells will facilitate the recovery of live-attenuated serotype I FIPV strains and highlight the importance of a genetically-malleable cell line to isolate clinical strains of serotype I FIPV from infected cats.

2. Results

Evaluating the interferon response in AK-D and IFNαR2-deficient AK-D 2.2 cells. We first targeted the type I interferon receptor (IFNαR) in an immortalized cell line derived from feline lung tissue (AK-D) using Crispr/Cas gene editing. AK-D cells were chosen because they are permissive to the serotype I FIPV Black strain used here and have a defined genotype. To disrupt the IFNαR2, wild-type AK-D cells were transduced with lentiviruses carrying a pLentiCRISPRv2 on which a single-guide (sg) RNA, targeting exon 2 of feline *ifnar2* (2.2), was encoded. Positive selection was performed using puromycin and surviving cells were cultivated as a polyclonal population termed AK-D 2.2. As there is no available IFNαR-specific antibody to detect the presence of feline IFNαR2 protein, we used a functional assay to evaluate the AK-D 2.2 cells for an IFN signaling-deficient phenotype. Increasing concentrations of purified feline IFNα were exogenously applied to AK-D or AK-D 2.2 cells and levels of IFN-stimulated gene (ISG) 54 transcript were determined by quantitative PCR (qPCR). ISG54 expression is prominently upregulated following activation of the type I IFN receptor (Fensterl and Sen, 2011) and is used here to report on the functionality of the IFNαR. As expected, parental AK-D cells responded to exogenous IFNα with a dose-dependent increase in ISG54 expression. The AK-D 2.2 cell population, however, produced significantly fewer ISG54 transcripts than the parental AK-D cells (Fig. 1A), indicating a disruption of the type I IFN response pathway. The subtle, yet concentration-dependent ISG54 transcription observed from AK-D 2.2 cells may be attributed to the polyclonal nature of the AK-D 2.2 cell population, which were selected for positive transduction, but not necessarily loss of IFN signaling. Nonetheless, these results indicate that the AK-D 2.2 cells have a diminished total response to IFNα, likely due to disruption of the IFNαR2.

Evaluating growth kinetics of serotype I FIPV Black in AK-D 2.2 cells. To determine if disrupting the IFNαR2 had an effect on replication of FIPV Black we evaluated the viral growth kinetics in AK-D and AK-D 2.2 cells. Virus titers were determined by plaque assay of cell-free supernatants derived from cells infected with FIPV Black at a multiplicity of infection (MOI) of 0.1. FIPV Black achieved a maximum titer $> 10^6$ plaque-forming units (PFU)/mL in both cell types. The kinetics of FIPV Black were similar in AK-D and AK-D 2.2 cells (Fig. 1B), with both cell types producing peak titers at 42 h post-infection (HPI), suggesting that the IFNαR2 does not significantly impact virus growth in this cell type. This was expected as FCoVs encode multiple IFN antagonists, which permit replication in AK-D cells independent of an IFN response (Dedeurwaerder et al., 2014, 2013).

Determining the utility of the AK-D 2.2 cells in visualizing FIPV Black plaques. Next, we asked if AK-D 2.2 cells can be used as an indicator cell type to accurately determine FIPV Black titer by plaque assay, a point of critical importance in future studies characterizing HIS mutant FIPV strains. An ideal indicator cell type allows a virus to form well-defined and easily enumerable plaques; therefore, we sought to determine if virus-induced cytopathic effect (CPE) or plaque size are affected by the absence of IFNαR2 in AK-D 2.2 cells. To evaluate CPE progression, AK-D and AK-D 2.2 cells were infected with 0.1 MOI FIPV Black. Over 48 h, we observed increased CPE in AK-D 2.2 cells compared to parental AK-D cells (**data not shown**), suggesting an increase in virus spread. To evaluate plaque formation, plaque assays were performed using a known concentration of FIPV Black, which was serially diluted and applied to AK-D and AK-D 2.2 indicator cells. FIPV Black formed large and enumerable plaques in AK-D 2.2 cells, which allowed for more accurate determination of virus titer compared to the parental AK-D cells (Fig. 1C). In AK-D 2.2 cells, plaques were more easily identified at 72 hpi, and plaque sizes were comparable to those on Fcwf-4 CU cells at 48 hpi as we recently reported (O'Brien et al., 2018). It was difficult to accurately determine virus titer using wild-type AK-D cells, as the plaques were too small to count accurately at both time points and led to an underestimation of PFU/mL. Our results highlight the utility of the AK-D 2.2 cells in determining the titer of serotype I FIPV and indicate that this cell line will be critical in future studies investigating IFN antagonist-mutant strains of FIPV.

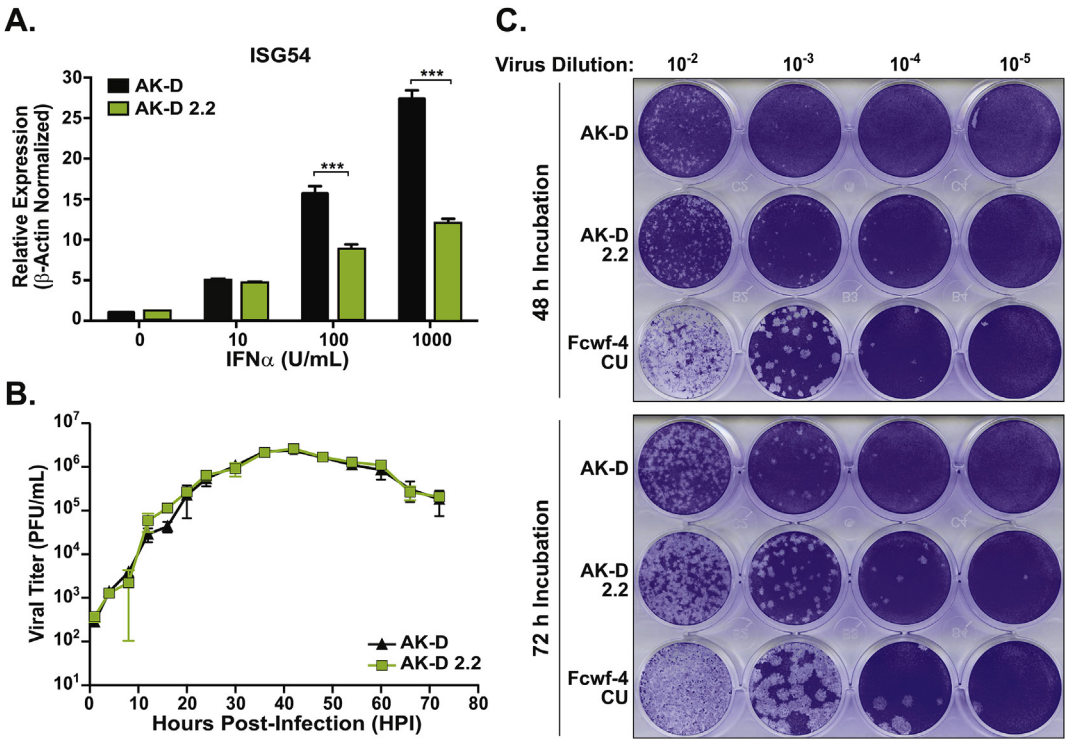

Fig. 1. Determining the response of AK-D 2.2 cells to type I interferon and characterizing the replication kinetics and plaque formation of FIPV Black in AK-D 2.2 cells. A) AK-D (black) or AK-D 2.2 (green) cells were treated with increasing concentrations of feline interferon alpha (IFNα). After 6 h, total RNA was extracted and analyzed by qPCR for ISG54 and feline *β*-actin. ISG54 mRNA expression was normalized to *β*-actin then presented as average $2^{-\Delta Ct}$ values. **B)** Growth kinetics of FIPV Black (MOI = 0.1) determined by plaque assay of infected AK-D (black) and AK-D 2.2 (green) cell supernatants. Data representative of two to three independent experiments performed in triplicate and presented mean ± SD. Values were analyzed by unpaired *t*-tests. ***P < 0.001. **C)** Fcwf-4 CU cells were infected with MOI = 0.1 serotype I FIPV Black and supernatants were collected at 24 HPI after which plaque assay analysis was performed on AK-D, AK-D 2.2, or Fcwf-4 CU indicator cells. Images were taken at 48 (top) and 72 (bottom) HPI. Images are representative of three independent experiments.

Disrupting IFN signaling in Fcwf-4 CU cells and evaluating the IFN-responsiveness and FIPV Black replication kinetics in an isolated clone. In addition to disrupting IFN signaling in AK-D cells, we also targeted the IFNαR2 in the feline macrophage-like cell line, Fcwf-4 CU. These cells are a more physiologically relevant cell type in which to study FIPV and grow the Black strain to high, cell-free titers (O'Brien et al., 2018). To knock down the IFNαR2, parental Fcwf-4 CU cells were transduced with lentiviruses carrying pLentiCRISPRv2 encoding an sgRNA targeting the second exon of the feline *ifnar2* gene (2.2), the same sequence targeted in AK-D cells. Positive transductants were selected using puromycin and cells were cultivated as a polyclonal population termed Fcwf-4 2.2 Poly. To evaluate the type I IFN-responsiveness of the Fcwf-4 2.2 Poly cells, cultures were treated with 1000 U of feline type I IFN for 6 h and evaluated for expression of ISG54. Compared to the parental Fcwf-4 CU cells, the Fcwf-4 2.2 Poly cells had reduced ISG54 transcript production suggesting positive disruption of the *ifnar2* gene (Fig. 2A). Next, in order to obtain a single, genetically-defined cell line, the Fcwf-4 2.2 Poly cells were sorted into a 96-well plate at one cell per well, and grown for 30 days. Three isolated clones (CL1-3) were evaluated for IFN-responsiveness by first stimulating with 1000 U of IFN then measuring levels of ISG54 transcript by qPCR (Fig. 2A). Fcwf-4 2.2 Poly clone 3, which exhibited the most subtle ISG54 response, were termed "IRN" for **I**FNα **R**eceptor **N**ull and maintained for further analysis. FIPV Black replication kinetics were similar in the parental Fcwf-4 CU and Fcwf-4 IRN clonal cell line as determined by plaque assay measuring infectious particles (Fig. 2B) and by qPCR measuring production of nucleocapsid (N) gene transcript (Fig. 2C). To further evaluate IFN responsiveness, Fcwf-4 CU and IRN cells were treated with 1000 U of type I IFN for 8 h prior to infection with FIPV Black (MOI = 0.01). As expected, virus replication was significantly reduced in parental CU cells pre-treated with IFNα (Fig. 2D). In contrast, pre-treatment of IRN cells with IFNα did not negatively impact virus replication (Fig. 2D) thereby providing further support of the IFNαR-null phenotype in this cell line. Lastly, we evaluated plaque size differences formed during FIPV Black replication in CU and IRN cells. Similar to what we observed with AK-D 2.2 cells, FIPV Black formed significantly larger plaques at days 3–4 post-infection in the IFNαR-null IRN cells compared to parental CU cells (Fig. 2E and F). Together, these results describe the successful generation and isolation of an IFNα response-deficient Fcwf-4 CU cell line, which will be highly useful in the recovery and study of IFN-antagonist mutant FCoVs in future studies.

Determining how IFN signaling is disrupted in Fcwf-4 IRN cells. Crispr/Cas gene editing targets and cleaves a specified nucleotide sequence leading to non-homologous end joining (NHEJ) DNA repair. This naturally imperfect double-strand break reconstruction process commonly introduces in/del mutations, which can disrupt gene transcription, reduce protein function or cause early termination of protein translation. We reasoned that the most direct method to determine how the IFNαR2 gene may be disrupted was to compare the *ifnar2* mRNA sequences produced in Fcwf-4 CU and IRN cells. Indeed, we found that the *ifnar2* mRNA obtained from Fcwf-4 IRN cells contained a 14-nucleotide deletion at the intended Cas9 cleavage site (Fig. 3A). The frameshift arising from this deletion positioned a stop codon in-frame, resulting in early termination at residue 27 and, likely, a shortened IFNαR2 protein (Fig. 3A). Further, we asked if *ifnar2* transcription was affected by this mutation. We found that mRNA expression from *ifnar2* exon 1–4, the region targeted by our sgRNA sequence, was actually higher in IRN cells compared to parental cells (Fig. 3B) indicating that disruption did not negatively impact transcription. Finally, we determined that the melting temperatures of the parental and IRN *ifnar2* exon 1–4 mRNA amplicons produced during qPCR differed, on average,

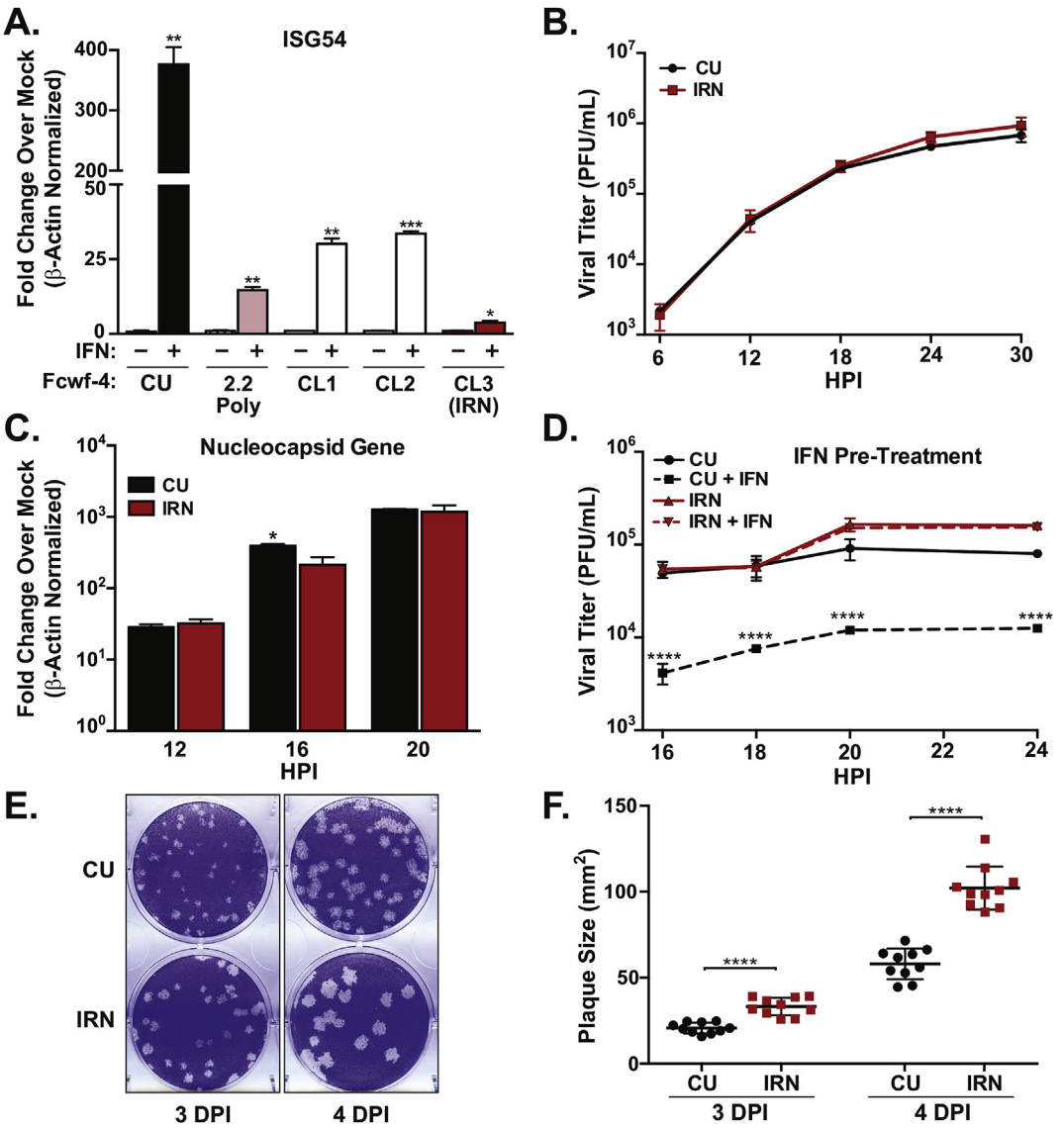

Fig. 2. Evaluating the response to type I interferon and the kinetics of FIPV Black replication in Fcwf-4 parent and IFNαR-deficient cells. A) Fcwf-4 CU, Fcwf-4 CU 2.2 Poly, Fcwf-4 CU 2.2 clones 1, 2 and 3 (IRN cells) were treated with 0 or 1000 U feline IFNα for 6 h and ISG54 transcripts were measured by qPCR. **B)** FIPV Black growth kinetics (MOI = 0.1) at indicated hours post-infection (HPI) in Fcwf-4 CU and IRN cells. **C)** Nucleocapsid gene transcript levels measured by qPCR during FIPV Black infection (MOI = 0.1) of Fcwf-4 CU or IRN cells. **D)** FIPV Black growth kinetics (MOI = 0.01) in indicated cells pre-treated with 0 or 1000 U feline IFNα for 8 h. **E)** Plaque formation induced by FIPV Black in Fcwf-4 CU or IRN cells at 3–4 days post-infection (DPI). Wells display $10^{-}5$ virus dilution. **F)** Plaque sizes (mm^2) measured from FIPV Black plaque assays (6-well plates) at 3 and 4 DPI on Fcwf-4 CU and IRN indicator cells at $10^{-}5$ and $10^{-}6$ virus dilutions. For mRNA expression, Ct values were normalized to β-actin using the $2^{-\Delta Ct}$ method and presented as fold expression over mock (A) or relative expression (B). Data represent 3 independent experiments in triplicate. Mean ± SD analyzed by unpaired t-tests. Viral titers (B and D) were calculated from triplicate plaque assays per time point on Fcwf-4 CU indicator cells and represent 3 independent experiments. Mean ± SD plaque-forming units (PFU) per mL analyzed by two-way ANOVA by time (D). Plaque sizes (F) were measured using Adobe Photoshop software and mean ± SD values were analyzed using unpaired t-tests. *P < 0.05; **P < 0.01; ***P < 0.001; ****P < 0.0001.

by 1 °C (Fig. 3C) further confirming a difference in the nucleotide composition (Krenke et al., 2005). Thus, the defect in IFN-responsiveness observed in Fcwf-4 IRN cells is likely the result of reduced function of a truncated IFNαR2 protein.

Expression of feline TMPRSS2 improves FIPV Black replication. Host-cell proteases are critical to coronavirus entry and can determine tissue tropism and replication efficiency (Millet and Whittaker, 2015). The transmembrane serine protease 2, TMPRSS2, has been shown to mediate or enhance cell-surface entry of a number of CoVs including human coronavirus (HCoV) 229E (Bertram et al., 2013; Shirato et al., 2016), Middle East respiratory syndrome (MERS)-CoV (Park et al., 2016; Shirato et al., 2013) and severe acute respiratory syndrome (SARS)-CoV (Glowacka et al., 2011; Reinke et al., 2017). As one of the goals of this study was to develop tools to aid in investigating feline coronavirus, we asked if expression of this protease could enhance FCoV replication. Feline TMPRSS2 protein carrying a C-terminal V5 tag was cloned into a pLVX lentivirus backbone vector and termed pLVX-fTMPRSS2(V5). To demonstrate subcellular localization and to visualize expression, HEK 293T/17 cells were transfected with the pLVX-fTMPRSS2(V5). The V5 epitope was detected by immunofluorescence within the cell cytoplasm and at the cell surface (Fig. 4A) and both the full-length (55 kDa) and the cleavage product (> 25 kDa), indicating an active protein, were detected from these cells by Western blot (Fig. 4B, **left**). Fcwf-4 IRN cells transduced with pLVX-fTMPRSS2(V5) lentivirus also had detectable levels of the full-length and active forms of TMPRSS2 (Fig. 4B, **right**) demonstrating that expression of an active

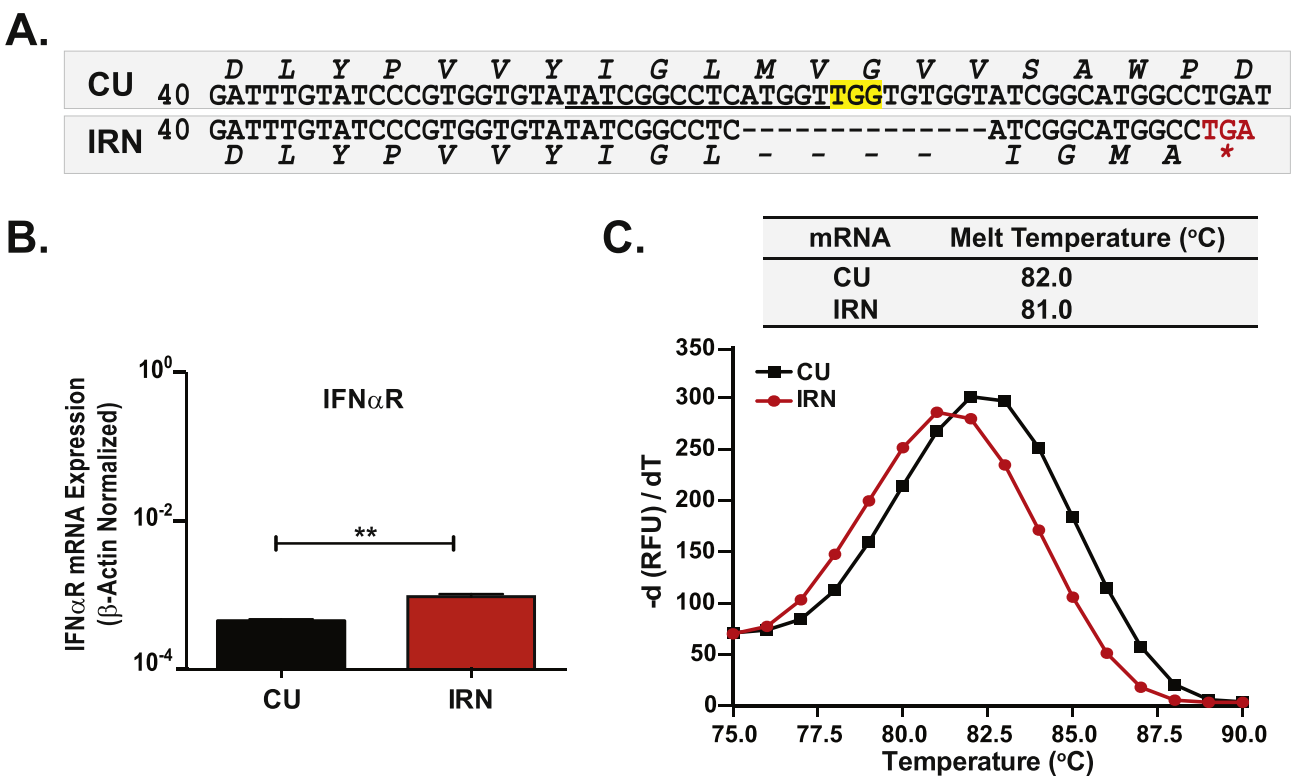

Fig. 3. Fcwf-4 IRN cells express an mRNA predicted to generate a truncated, null-mutant IFNαR protein. A) Deduced nucleotide and amino acid sequences of the IFNαR2 region targeted by Crispr/Cas technology. Single-guide RNA sequence target (underlined); protospacer-adjacent motif (PAM) (yellow); STOP codon and asterisk (red) indicate early termination of translation of the IFNαR2 protein in IRN cells. **B)** Feline IFNαR2 exon 1 expression determined from total RNAs collected from Fcwf-4 CU and Fcwf-4 IRN confluent monolayers. mRNA expression normalized to β-actin and presented as average $2^{-\Delta Ct}$ expression values. Data represent two independent experiments in triplicate. Mean ± SD analyzed by unpaired t-tests. **P < 0.01. **C)** Melt curves and maximum melt temperatures of IFNαR2 amplicons produced during qPCR of RNAs obtained from Fcwf-4 CU or Fcwf-4 IRN cells. (For interpretation of the references to colour in this figure legend, the reader is referred to the Web version of this article.)

feline protease was achievable in this cell line. Therefore, we sought to determine if TMPRSS2 had an impact on the replication of FIPV. Fcwf-4 IRN cells were transduced with increasing dilutions of pLVX-fTMPRSS2(V5) lentivirus for 48 h, then infected with FIPV Black at a MOI of 0.1 for 18 h. Expression of TMPRSS2 at dilutions below 1:20 (Fig. 4C) resulted in significant increases in FIPV N gene transcript (Fig. 4D) compared to cells that did not express TMPRSS2, suggesting that addition of a feline protease can enhance virus replication. Interestingly, N gene expression was reduced at lower dilutions of TMPRSS2 (1:2.5) suggesting that expression of these proteases needs to be carefully titrated, and too much protein can result in reduced titers. Together, these data describe the successful generation of two IFNαR-null cell lines by Crispr/Cas, the isolation of an Fcwf-4 IFNαR-null clone, and demonstrate that expression of a feline protease in these cells can enhance replication of serotype I FIPV.

3. Discussion

The future goal of developing and evaluating live-attenuated serotype I FCoV vaccine strains may be possible through mutation of encoded IFN antagonists (Deng et al., 2019, 2017; Kindler et al., 2017; Menachery et al., 2018). Feline cell lines that lack IFN signaling are necessary for generating these potential FCoV vaccine strains in order to avoid selective pressures that would reduce or eliminate virus replication. To our knowledge, such IFN-nonresponsive feline cell lines were not available and studies using gene-modifying tools such as Crispr/Cas had not been performed in feline cells permissive to FCoVs. In a previous study, we characterized the growth kinetics of FIPV Black in AK-D and Fcwf-4 CU cells and demonstrated that rapid growth of wild-type serotype I FIPV could be achieved given the right cell type and conditions (O'Brien et al., 2018). However, these cells still produced IFN upon stimulation suggesting that neither cell line would be appropriate for recovery of viruses attenuated by deletion on IFN antagonists. Previous studies from our lab using mouse hepatitis virus (MHV), a model murine coronavirus, strongly imply that production of IFN antagonist-deficient CoVs by reverse genetics absolutely requires the use of an IFN-nonresponsive cell type (Deng et al., 2017). In that study, we determined by deep-sequencing that mutant MHV strains produced in IFN-responsive cells acquired additional suppressor mutations. This phenomenon likely occurred in response to selection imposed by the antiviral activity of type I IFN, which may have selected against the attenuated phenotype. Cells lacking IFNαR allowed for recovery of "clean" mutant viruses that contained only the desired mutation. Subsequent characterization of novel MHV IFN antagonists, as well as the relevant mechanisms underlying their activities, were undertaken using IFNαR$^{-/-}$ cells, highlighting the need of such cell lines in investigating attenuated FCoV strains. Building on this idea, the goal of this study was to genetically modify AK-D and Fcwf-4 CU cells to generate cell lines that are i) highly permissive to serotype I FCoV and ii) deficient in IFNαR signaling, two characteristics we predict will allow future investigation of not only HIS viruses, but also isolation of clinically important FIPV strains.

The AK-D 2.2 and Fcwf-4 IRN cells generated in this study provide an initial, yet critical reagent necessary to isolate novel FCoV strains that do not express IFN antagonists, termed hyper interferon sensitive (HIS) viruses (Du et al., 2018). Both of the newly developed cell types display the desired characteristics, exhibiting a deficiency in IFN responsiveness while remaining highly permissive to FIPV Black infection. We demonstrated that the AK-D 2.2 and Fcwf-4 IRN cells permitted virus replication to high titers similar to those obtained from

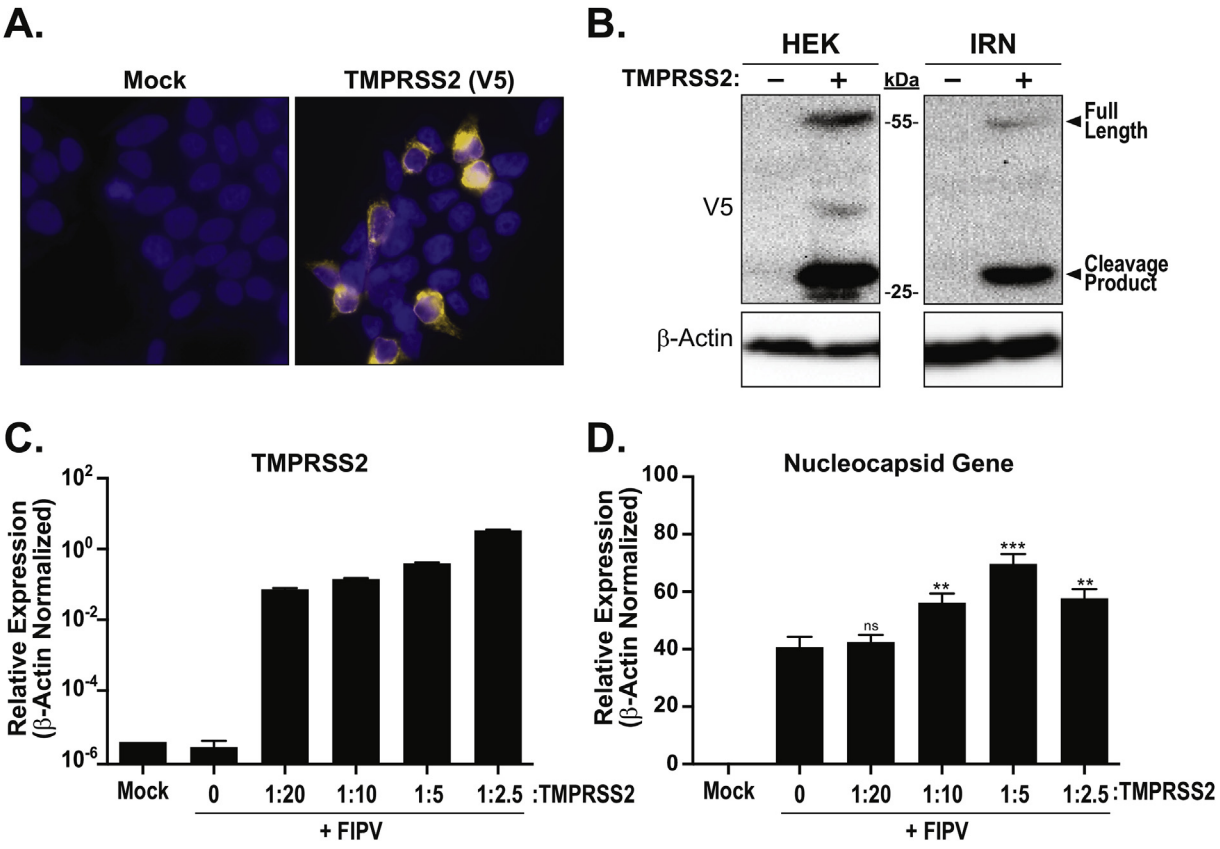

Fig. 4. Expressing TMPRSS2 in feline cells and evaluating the effect on FIPV Black replication. A) Immunofluorescence detection of feline TMPRSS2(V5) in HEK 293T/17 cells. 200 ng of pLVX-fTMPRSS2(V5) or pLVX (mock) was transfected into HEK 293T/17 cells for 18 h. Cells were stained with mouse-anti-V5 (1:500), and 1:1000 Alexa Flor 568-conjugated goat-anti-mouse IgG was used to visualize TMPRSS2(V5); Hoesch 3342 (1:1000) was used to stain nuclei. **B)** Detection of feline TMPRSS2(V5) by Western blot following transfection of HEK 293T/17 cells (left) or transduction of Fcwf-4 IRN cells with pLVX lentiviruses encoding TMPRSS2(V5) (right). The full length (55 kDa) and cleavage product (> 25 kDa) of TMPRSS2 are indicated. Feline β-actin used to visualize protein loading. **C-D)** The impact of feline TMPRSS2 expression on FIPV replication evaluated in Fcwf-4 IRN cells. Indicated dilutions of pLVX-fTMPRSS2(V5) or Mock (empty) transducing particles were applied to Fcwf-4 IRN cells for 48 h prior to infection with FIPV Black (MOI = 0.1). RNA was isolated after 18 h infection and qPCRs were performed to detect TMPRSS2 **(C)**, N gene **(D)**, and β-actin transcripts. mRNA expression normalized to β-actin and presented as average $2^{-\Delta Ct}$ expression values. Data represent two independent experiments in triplicate. Mean ± SD analyzed by unpaired t-tests. **P < 0.01; ***P < 0.001; not significant (ns).

infected parental cells. These results were expected as wild-type FCoVs encode IFN antagonists allowing virus replication despite the potent antiviral activities of type I IFN (Dedeurwaerder et al., 2014, 2013). The Fcwf-4 IRN clonal cell line will be an important tool moving forward as these cells have low IFN-responsiveness due to a defined IFNαR2 mutation, grow high titers of FIPV Black, and can be effectively transduced to express additional host proteins. The AK-D 2.2 cells were shown to be useful in determining virus titer by plaque assay. FIPV Black induced more rapid CPE development in AK-D 2.2 compared to parental AK-D cells, resulting in larger and more easily enumerable plaques. This same trend was observed in Fcwf-4 cells, with virus forming larger plaques in IRN cells compared to CU cells. We speculate that these larger plaques may develop due to increased virus spread into adjacent uninfected cells due to lower expression of antiviral ISGs in the IFNαR-disrupted cell populations. Importantly, the ability of serotype I FIPV to form larger plaques on AK-D 2.2 and Fcwf-4 IRN cells allows more accurate titer determination and will be critical in future studies to accurately measure the titer of HIS FCoVs.

The final objective of this study was to determine if we could enhance the replication of serotype I FIPV in IRN cells, which may aid in the recovery of IFN sensitive strains in future studies. TMPRSS2, a transmembrane serine protease, has been shown to promote entry of many coronaviruses into host cells (Bertram et al., 2013; Glowacka et al., 2011; Park et al., 2016; Reinke et al., 2017; Shirato et al., 2016, 2013). While tropism of FCoV has been linked to protease usage (Licitra et al., 2013), many details remain to be determined. To demonstrate the utility of the clonal Fcwf-4 IRN cell line in investigation of type I FCoVs, we transduced these cells with feline TMPRSS2 as a surrogate protease and observed a significant, though modest, increase FIPV Black replication as detected by an increase in N gene expression. This is an important observation as it demonstrates that Fcwf-4 IRN cells can be transduced to express functional proteins, and that addition of host factors is a viable way of enhancing serotype I FIPV infection in these cells. It should be noted that both infected and uninfected Fcwf-4 IRN cells that were transduced with the 1:2.5 dilution of lentivirus had significant morphologic differences, such as increased cell rounding, clumping and detachment from the plate, compared to higher dilutions and non-transduced cells. Lower N gene expression, indicating reduced virus titer, was also observed in cells with the highest TMPRSS2 expression. This may be due to reduced accessibility of the virus to cells that were not adherent to the dish, or alternatively, the increased abundance of active TMPRSS2, which may prematurely cleave CoV spike, preventing efficient membrane fusion and cell entry.

An additional benefit to TMPRSS2-expressing Fcwf-4 IRN cells is their potential to recover serotype I FIPV isolates directly from clinical samples. CoV spike-mediated membrane fusion and subsequent entry into host cells has been shown to occur at both the cell surface and within endosomes depending on the availability of host proteases (Belouzard et al., 2012; Millet and Whittaker, 2015) (Fig. 5, **top**). For serotype I FCoVs, the presence of a furin cleavage site at S1/S2 is linked

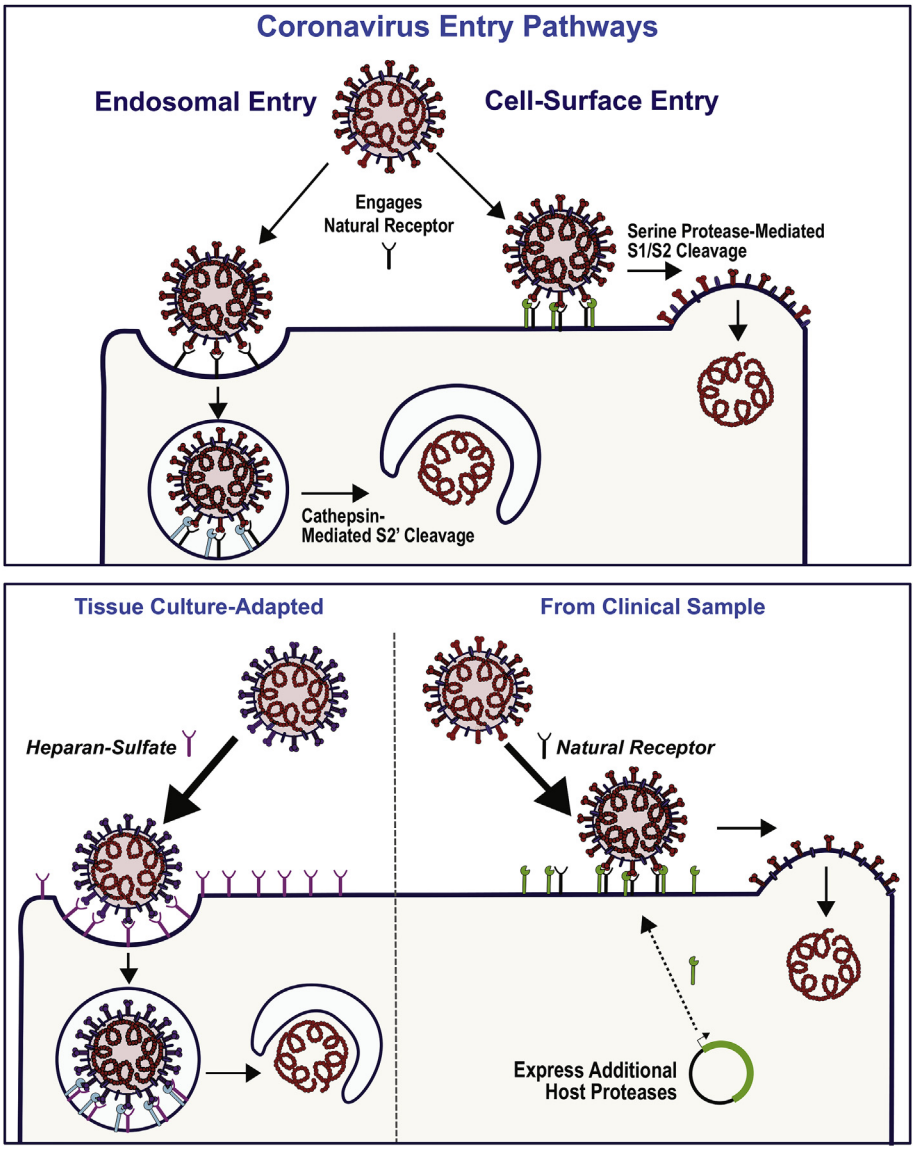

Fig. 5. Proposed model for IRN cells expressing TMPRSS2 for the recovery of serotype I FIPV from clinical samples. Serotype I FIPV entry likely occurs within endosomes via cathepsin [cyan] cleavage of the CoV spike at S2′ or at the cell surface via protease cleavage of S1/S2 following S engagement of the natural receptor (black) **(top)**. The proposed models for tissue culture-adapted FCoV entry and recovery of serotype I FIPV from clinical samples are depicted in the lower panel. Tissue culture-adapted strains may express spikes (violet) that lose S1/S2 cleavage in favor of heparin (magenta) binding **(bottom left)**. Expressing host factors, such as TMPRSS2 (green), may promote natural receptor usage and cell-surface entry, aiding in recovery of serotype I FCoV strains from clinical samples **(bottom right)**.

to both clinical outcome and cell culture adaptation, while cleavage at the S2' site likely mediates entry within endosomes. For FIPV Black, we consider that the presence of a trypsin-like protease (e.g. TMPRSS2) at the cell surface can functionally replace the usual endogenous protease to promote virus replication. Importantly, entry of serotype I FCoV can be further impacted by tissue culture (TC) adaptation. de Haan and colleagues demonstrated that the spike protein encoded on a Fcwf-4 TC-adapted serotype I FCoV strain, FIPV-UCD1, had reduced cleavage at the S1/S2 site, but exhibited increased binding to heparan sulfate (de Haan et al., 2008). Interestingly, the serotype I FCoV clinical isolate, FECV-UCD, contains a full furin cleavage site at S1/S2 and did not bind heparan sulfate, and therefore did not replicate in Fcwf-4 cells. This suggests that TC-adapted strains may forfeit S1/S2 cleavage along with binding to heparan sulfate, possibly a more abundant entry receptor on Fcwf-4 cells compared to the yet unknown natural receptor for serotype I FCoV (Fig. 5**, bottom left**). The concept that TC-adaptation can alter the preferred virus entry pathway may be common amongst lab-adapted CoV strains. A recent study by Shirato et al. showed that clinical isolates of HCoV 229E, much like serotype I FCoV clinical strains, favored TMPRSS2-mediated cell-surface entry while high passage, TC-adapted strains preferentially adopted cathepsin-mediated entry in endosomes (Shirato et al., 2016).

We speculate that the cells and protease expression studies described here may provide an approach for recovery of additional pathogenic strains of serotype I FCoV from infected cats and lay the groundwork for future experiments and discussion. If serotype I FCoV growth in Fcwf-4 cells positively selects for the use of heparan sulfate as an entry receptor, and by extension the loss of the furin site, then this may explain why TC-adapted strains lose pathogenicity. Cell-surface level entry, mediated by S1/S2 cleavage by TMPRSS2, has been shown to be involved in pathogenicity and spread of CoVs in vivo (Park et al., 2016; Shirato et al., 2013) possibly by increasing the kinetics of virus entry (Earnest et al., 2017). Therefore, the change in the S1/S2 cleavage site in TC-adapted strains may significantly contribute to both a loss of pathogenicity and an inability to cultivate true clinical isolates without several rounds of passage. Interestingly, serotype II FCoVs do not contain an S1/S2 cleavage site, do not apparently utilize heparan sulfate, and use feline aminopeptidase N (fAPN), a different entry receptor than serotype I FCoV (Hohdatsu et al., 1998). As such, TC adaptation of serotype II FIPV strains does not typically correspond with a loss in pathogenicity (Tekes et al., 2012; Thiel et al., 2014) suggesting that maintenance of the natural receptor-entry route may allow recovery of pathogenic type I strains. Thus, increasing the expression of S1/S2-targeting host enzymes such as TMPRSS2 may lead to more efficient recovery of clinical type I FIPV strains (Fig. 5**, bottom right**).

Together, the results presented here describe the successful

disruption of the IFNαR in two feline cell lines and suggest that overexpression of feline proteases, in at least one of these cell lines, may be useful for enhancing infection of serotype I FCoVs. Importantly these data also demonstrate the genetic malleability of the Fcwf-4 CU cells and, to our knowledge, represent the first genetically-modified Fcwf-4 cell line. Thus, both the AK-D 2.2 and the Fcwf-4 IRN cells will be useful in future studies evaluating feline viruses that lack IFN antagonists and may be an important tool for isolating serotype I FCoVs from clinical samples.

4. Materials and methods

Cell lines. AK-D cells, which are immortalized cells derived from feline lung tissue, were purchased from the American Type Culture Collection (ATCC) (ATCC® CCL-150™) and maintained in Dulbecco's Modified Eagle Medium (DMEM; Gibco, #12100-046) containing 10% fetal bovine serum (FBS) (Atlanta Biologicals, #S11150), supplemented with 2.2 g/L of sodium bicarbonate (Sigma, #S5761), 1% non-essential amino acids (HyClone, #SH30238.01), 1% HEPES (HyClone, #SH30237.01), 1% sodium pyruvate (Corning, #25-000-CI), 1% L-glutamine (HyClone, #SH30034.01), and 1% penicillin/streptomycin (Corning, #30-002-CI). AK-D 2.2 cells were also maintained in this medium. *Felis catus* whole fetus cells were provided by Dr. Edward J. Dubovi, Cornell University College of Veterinary Medicine, Ithaca, NY, and designated Fcwf-4 CU. Fcwf-4 CU cells were maintained in Eagle's Minimal Essential Medium (EMEM) (Sigma, #M0268) containing 10% FBS, supplemented with 1.5 g/L sodium bicarbonate, 1% non-essential amino acids, 1% HEPES, 1% sodium pyruvate, 1% L-glutamine and 1% penicillin/streptomycin. Fcwf-4 2.2 Poly and Fcwf-4 IRN cells were also maintained in this medium. Human embryonic kidney (HEK) 293T/17 cells (ATCC® CRL-11268™) were maintained in DMEM (Corning, #10-017-CV) containing 10% FBS, supplemented with 1% nonessential amino acids, 1% HEPES, 1% L-glutamine, 1% sodium pyruvate, and 1% penicillin/streptomycin. For passaging, confluent cell monolayers were rinsed with PBS, lifted by addition of 2 mL of 0.25% trypsin (Gibco, #15090-046) in versene solution (0.48 mM EDTA in PBS) then transferred (split 1:5 or 1:10) to a new T-75 flask in complete media every 2–3 days.

Viruses. Serotype I feline infectious peritonitis virus (FIPV) Black (TN-406) was kindly provided by Dr. Fred Scott, Cornell University College of Veterinary Medicine, Ithaca, NY. FIPV Black was propagated in Fcwf-4 CU cells and recovered from supernatants for stock virus preparation. Briefly, sub-confluent T-75 flasks of Fcwf-4 CU cells were infected with virus at a multiplicity of infection (MOI) of one for 1 h in 2 mL serum-free media at 37 °C and 5% CO_2. Infectious media was replaced with 10 mL EMEM containing 2% FBS, and the monolayer was incubated at 37 °C and 5% CO_2. After 24 h, supernatants were collected and clarified by centrifuging at 1000 xg for 10 min at 4 °C. Virus-containing cell-free supernatants were then aliquoted (100–300 µL) and stored at −80 °C. Titers of stock virus were determined by plaque assay on AK-D or Fcwf-4 CU cells.

Generation of IFNαR2-disrupted AK-D and Fcwf-4 CU cell populations. A modified Crispr/Cas9 protocol, based on the GeCKO system (Shalem et al., 2014) was used to knock-out the function of the type I IFN alpha receptor 2 (IFNαR2) in AK-D and Fcwf-4 CU cells. Briefly, single-guide (sg) RNA sequences were identified using Benchling (Benchling, INC.) to target the second exon (felis_catus_6.2; range = cgrC2: 11959183–11979720) of the feline *ifnar2* gene (Accession NM_001278859.1). Complementary DNA versions of the sgRNAs (Fwd 5′- CAC CGT GTG TAT CGG CCT CAT GGT-3'; Rev 5′- AAA CAC CAT GAG GCC GAT ACA CAC-3′) were annealed and inserted into a pLentiCRISPRv2-puro (Addgene #52961) cassette between flaking BsmBI sites. To generate transducing particles (TPs), IFNαR2-specific or empty vector (EV), plasmid DNAs pLentiCRISPRv2-puro, pPax2 and pHEF-VSV-G plasmids were co-transfected into HEK-293T/17 cells using polyethylenimine in antibiotic-free DMEM containing 10% FBS for 24 h, followed by replacement with complete DMEM containing 10% FBS. After 48 h, supernatant containing TPs was centrifuged at 1000 x g for 10 min at 4 °C and filtered through a 0.45 µM filter (Millipore Sigma). TPs were applied to sub-confluent monolayers of parental AK-D or Fcwf-4 CU cells for 48 h followed by selection in DMEM containing 10% FCS and 25 µg/mL puromycin (InvivoGen) for 96 h. Puromycin-selected cells were grown and passaged as polyclonal populations designated AK-D 2.2 and Fcwf-4 2.2 Poly, respectively.

Clonal expansion and IFNαR2 sequencing of Fcwf-4 IRN cells. A clone of the Fcwf-4 2.2 Poly cells, confirmed for reduction in responsiveness to type I IFN, was isolated and designated Fcwf-4 IRN (**I**nterferon alpha **R**eceptor **N**ull). Briefly, > 10,000 Fcwf-4 2.2 Poly cells were sorted using a FACS Aria Cell Sorter (BD) into a 96-well plate at 1 cell/well. Clones were expanded into 24- then 6-well plates in EMEM containing 10% FBS and 10 µg/mL puromycin. Clones permissive to FIPV Black infection were evaluated for IFN responsiveness. The Fcwf-4 IRN cell line was isolated in this manner and confirmed to be both permissive to FIPV Black infection and have low IFN-responsiveness. The sequence of the IFNαR mRNA expressed in the Fcwf-4 IRN cell line was determined by sequencing 15 PCR clones of the region. Briefly, total RNA was isolated from Fcwf-4 CU or IRN cell monolayers and cDNA was generated with random hexamer primers via the RevertAID First-Strand cDNA Synthesis kit (Thermo Fisher). The full IFNαR mRNA sequence was PCR amplified from cDNA then inserted into TA cloning pCR-XL-TOPO® plasmids using the TOPO® XL PCR Cloning Kit (Life Technologies). Plasmids for each cell type were then purified by MiniPrep (Promega) and 15 from each cell type were sequenced. Consensus sequences were compared using Clone Manager 9 (Sci-Ed Software).

IFNα stimulation and detection of ISG54 gene transcripts by quantitative real-time PCR. Indicated feline cells were stimulated with purified feline IFNα (PBL Assay Science #15100-1) then assayed for the level of IFN stimulated gene 54 (ISG54) produced. Briefly, cells were plated in a 24-well plate (Corning) at 1.5 - 3.0 × 10^5 cells/well in 0.5 mL of DMEM containing 10% FBS for 24 h at 37 °C and 5% CO_2. Cells were treated with media (mock) or purified feline IFNα at 10, 100, or 1000 U/mL for 6 h. Cell were lysed in 350 µL RLT buffer and total RNA was purified using a RNeasy Mini kit (Qiagen). Using 1 µg purified total RNA, cDNA was generated via the RT^2 First-Strand cDNA Synthesis kit (Qiagen). qPCR was performed to determine abundance of feline β-actin (Fwd 5′-CAA CCG TGA GAA GAT GAC TCA GA-3'; Rev 5′-CCC AGA GTC CAT GAC AAT ACC A-3′) (Kessler et al., 2009) and feline ISG54 (Fwd 5′-CCT GAG CTG CAG CCT TTC AGA ACA G-3'; Rev 5′- CAC GTG AAA TGG CAT TTA AGT TGC CGC AG -3′) RNAs. ISG54 Ct values were normalized to *β*-actin and presented as average $2^{-\Delta CT}$ [$\Delta C_T = C_{T\ (gene\ of\ interest)} - C_{T\ (\beta\text{-}actin)}$] expression values or fold expression over mock.

Determining IFNαR2 expression and amplicon melt temperature. Expression and amplicon melt temperature of feline *ifnar* gene exons 1–4 were determined by qPCR. Briefly, confluent monolayers of Fcwf-4 CU and Fcwf-4 IRN cells were grown overnight in EMEM containing 10% FBS, lysed in RLT (Qiagen) and total RNA was isolated using the RNeasy RNA isolation kit (Qiagen). Equivalent amounts of RNA were used to generate cDNA using RevertAID cDNA synthesis kit (ThermoFisher). Feline *β*-actin (see above) and IFNαR2 exon 1–4 (Fwd 5′-AAG ATG CTT TGG AGC CAG AAT A-3'; Rev 5′- CCA GGA AGA AAT CGC TGA TAC A-3′) transcript levels were determined by qPCR using Sybr Green Master Mix (Qiagen). qPCRs were performed in a CFX96 thermocycler (Bio-Rad) using the following settings: 95 °C for 10 min; 40 cycles of 95 °C for 15 s, 58 °C for 1 min and SYBR read; 95 °C for 10 s; melt curve from 65 °C to 95 °C at 0.5 °C/0.5 s. For qPCR, samples were evaluated in triplicate and data represent three independent experiments. The levels of mRNA were normalized to *β*-actin mRNA and presented as average $2^{-\Delta CT}$ [$\Delta C_T = C_{T\ (gene\ of\ interest)} - C_{T\ (\beta\text{-}actin)}$] expression values. Melt temperatures were determined by plotting the change in fluorescence with temperature [-d(RFU)/dT] versus

temperature (°C) then calculating the point at which the largest change in fluorescence occurs (Krenke et al., 2005).

Plaque assay. The plaque assay technique was performed using AK-D, AK-D 2.2. Fcwf-4 CU, and IRN as indicator cells. Briefly, 6.5×10^5 cells per well were plated in 6-well plates or 3.0×10^5 cells per well were plated in 12-well plates. Cells were washed with PBS, then infected with 300 µL (6-well plate) or 150 µL (12-well plate) of 10-fold serial dilutions of viral samples in FBS-free media for 1 h at 37 °C. Cells were overlaid with a 0.5% Oxoid agar (Oxoid LTD, #LP0028)-DMEM containing 1% FBS. Plates were incubated at 37 °C for 48 h (or the indicated time) and fixed using 3.7% formaldehyde-PBS solution for 30 min. Viral plaques were visualized by staining with 0.1% crystal violet for 30 min. To quantify the plaque size, 10 isolated plaques from FIPV-infected CU cells and 10 isolated plaques from FIPV-infected IRN cells were measured using Adobe Photoshop software. The cleared area of the plaque was calculated in square millimeters.

Virus growth kinetics. We analyzed the growth kinetics of type I FIPV Black in five cell types: AK-D, AK-D 2.2, Fcwf-4 CU, Fcwf-4 2.2 Poly and Fcwf-4 IRN cells. For all cell types, 3.0×10^5 cells were plated in 12-well plates for 24 h. Cells were infected with FIPV Black in serum-free media at a MOI of 0.1 at 37 °C. After a 1 h, infectious media was replaced with media containing 2% FBS. Cell supernatants were collected from cultures at the times indicated and centrifuged at 2200 x g for 10 min at 4 °C to remove cells and cell debris, then aliquoted and frozen at −80 °C until use. Virus titers at each timepoint were determined by plaque assay, in triplicate, using either AK-D or Fcwf-4 CU indicator cells.

Virus growth kinetics in cells pre-treated with feline IFNα. Serotype I FIPV Black virus growth kinetics were evaluated in feline cells pre-treated with IFNα. Briefly, Fcwf-4 CU and Fcwf-4 IRN cells were plated in 24-well plates at 3.0×10^5 cells/well for 24 h, then treated with 0 or 1000 U feline IFNα (PBL Assay Science #15100-1) for 8 h. Cells were infected (as above) with FIPV Black in serum-free media at a MOI of 0.01 at 37 °C for 1 h and cultured in EMEM containing 2% FBS. Cell supernatants collected from cultures at indicated times were centrifuged at 2200 x g for 10 min at 4 °C to remove cells and debris. Virus titers were determined at each timepoint by plaque assay, in triplicate, using Fcwf-4 CU indicator cells.

Cloning and expression of feline TMPRSS2 in Fcwf-4 IRN cells. A dsDNA gBlocks® (IDT) fragment containing the coding sequence of feline TMPRSS2 variant 1 (GenBank accession # XM_023238709.1) was designed with several modifications for cloning into the pLVX-Puro vector. A Kozak consensus sequence was added to the 5′ end, while the 3′ end contains a 3 nt spacer sequence followed by an in-frame V5 tag coding region. The plasmid carrying this sequence was termed pLVX-fTMPRSS2(V5)-puroR$^+$. Transducing particles (TPs) carrying the pLVX-fTMPRSS2(V5)-puroR$^+$ plasmids were generated by transfecting 3.3 µg each of pLVX-fTMPRSS2(V5)-puroR$^+$, psPax2, and pHEF-VSV-G plasmid DNAs into 10 cm dishes containing 5.0×10^6 HEK-293T/17 cells using polyethylenimine (PEI) (5 µg PEI/1 µg DNA) in antibiotic-free DMEM containing 10% FBS for 24 h followed by replacement with DMEM containing 10% FBS with antibiotics. After 48 h, supernatants containing TPs were collected and stored at 4 °C and cells were replenished with 10 mL DMEM containing 5% FBS with antibiotics. After an additional 24-h incubation (72 h total) at 37 °C and 5% CO_2, supernatants were collected and combined with the previously collected lot. Total supernatants were centrifuged 1000 xg at 4 °C for 10 min to remove cell debris, then centrifuged for 16 h at 5000 x g and 4 °C. To concentrate, supernatants were poured off and pellets were suspended in one tenth the original volume using EMEM. For expression of feline TMPRSS2(V5), transducing particles were diluted 1:5 in serum-free EMEM and a minimal volume was incubated with Fcwf-4 IRN cells for 1 h at 37 °C and 5% CO_2 followed by addition of EMEM containing 6.25% FBS. After 48 h, cells were lysed in either lysis buffer A (4% sodium dodecyl sulfate, 3% dithiothreitol, 40% glycerol, and 0.065 M Tris-HCl pH 6.8) for evaluation of TMPRSS2(V5) by Western blot or lysed in RLT buffer (Qiagen) for evaluation of TMPRSS2 mRNA levels by qPCR. For Western blot, lysates were sonicated, and 5.0×10^4 cell-equivalents were separated through 7–15% acrylamide Mini-PROTEAN® TGX™ precast SDS-PAGE gels (Bio-Rad) then transferred to PVDF membranes using a semi-dry Trans-Blot® Turbo™ transfer system (Bio-Rad). Membranes were blocked at 4 °C overnight in 5% milk in TBST followed by 90 min room temperature incubation in primary antibodies specific for TMPRSS2(V5) tag (murine anti-V5 monoclonal IgG; Fisher Scientific #R96025) or β-actin (murine anti-actin monoclonal IgG; Genscript #A00702-40) diluted 1:2500 and 1:5000, respectively, in 5% milk-TBST. Membranes were washed in TBST then incubation for 1 h at room temperature in horseradish peroxidase (HRP)-conjugated goat-anti-mouse IgG (SouthernBiotech) secondary antibody diluted 1:5000 in 5% milk-TBST. Western Lightning® Plus-ECL (PerkinElmer, Inc.) chemiluminescent substrate was applied to washed membranes and bands were visualized on a FluorChem™ E (Protein Simple) imaging system relative to PageRuler™ Prestained protein ladder (Thermo Fisher). For detection of feline TMPRSS2 mRNA transcript levels, qPCRs were performed. Briefly, total RNA was extracted from RLT lysates using a RNeasy Mini Kit (Qiagen) and 500 ng RNA was used for cDNA synthesis using RT^2 HT First-Strand Kit (Qiagen, #330401). qPCR was performed with specific primers for feline TMPRSS2 (Fwd 5′-TGT CTA CAA CAA CCT GGT CAC-3'; Rev 5′-CCA CCA GAT GTG ACT CTT CAT AG-3′) or feline β-actin transcript (see above) using RT^2 SYBR Green qPCR Mastermix (Qiagen, #330502). A Bio-Rad CFX96 thermocycler was set as follows: one step at 95 °C (10 min); 40 cycles of 95 °C (15 s), 58 °C (1 min), and plate read; one step at 95 °C (10 s); and a melt curve from 65 °C to 95 °C at increments of 0.5 °C/0.5 s. Samples were evaluated in triplicate and data are representative of three independent experiments. Levels of mRNA were normalized to β-actin mRNA and presented as average $2^{-\Delta CT}$ [$\Delta C_T = C_{T\ (gene\ of\ interest)} - C_{T\ (\beta\text{-}actin)}$] expression values.

Detection of TMPRSS2(V5) protein. An immunofluorescence assay was used to detect expression of feline TMPRSS2(V5) in HEK 293T/17 cells following transfection. Briefly, 200 ng of pLVX-fTMPRSS2(V5) or pLVX (mock) was transfected into sub-confluent monolayers of HEK 293T/17 cells, grown on coverslips, for 18 h. Cells were then fixed with 3.7% formaldehyde-PBS solution, permeabilized with 0.1% Triton X-100, and blocked overnight in 5% normal goat serum (NGS)/0.3% Triton X-100 in PBS. Cells were then stained with mouse-anti-V5 (1:500) for 1 h at room temperature with rocking and washed three times in PBS. A secondary antibody, Alexa Fluor 568-conjugated goat anti-mouse IgG (Thermo Fisher Scientific, #A11004) was then applied at a dilution of 1:1000 in the presence of Hoechst33342 (Thermo Fisher Scientific, #H1399) at a dilution of 1:1000 for nucleus staining. After 30 min incubation with the secondary antibody at room temperature, the cells were washed with PBS, mounted onto slides using Fluoro-gel and examined under a fluorescence microscope. Images were processed using Image-J software (Wayne Rasband, NIH). All antibodies were diluted using 0.5% NGS/0.3% Triton X-100 in PBS.

Detecting FIPV N gene in FIPV-infected Fcwf-4 IRN cells expressing TMPRSS2. To determine effects of TMPRSS2 on FIPV replication, Fcwf-4 IRN cells were transduced with increasing dilutions of lentiviruses expressing TMPRSS2 then infected with FIPV Black. N gene expression was determined by qPCR. Briefly, 24-well Cell-Bind plates (Corning) were seeded with 0.5 mL Fcwf-4 IRN cells at 3.0×10^5 cells/mL in complete EMEM and incubated overnight at 37 °C and 5% CO_2. Media was replaced with 100 µL serum-free EMEM (mock), or cells were transduced with 100 µL fTMPRSS2(V5) lentivirus TPs left undiluted, or diluted 1:20, 1:10, 1:5 and 1:2.5 in serum-free EMEM. After 1 h incubation, 400 µL EMEM (6.25% FBS) was added to each well (without media replacement) to give 500 µL and 5% FCS. Cells were incubated for 48 h to allow expression of TMPRSS2 then infected with FIPV Black at a MOI of 0.1, or left uninfected (mock; mock expressing TMPRSS2). After an additional 18 h infection, cells were lysed in RLT

(Qiagen) and RNA was isolated using RNeasy Mini Kit (Qiagen). Equivalent amounts of RNA were used to generate cDNA using the RevertAID cDNA Synthesis Kit (ThermoFisher). FIPV Black N gene (Fwd 5′-ACC AGC CAA TTC CTA GAA CAG-3'; Rev 5′-GAA CGG GAT TTT CTT TGC CTC-3′) and β-actin (see above) transcript levels were determined by qPCR using Sybr Green Master Mix (Qiagen). qPCRs were performed in a CFX96 thermocycler (Bio-Rad) set to: 95 °C for 10 min; 40 cycles of 95 °C for 15 s, 58 °C for 1 min and SYBR read; 95 °C for 10 s; and a melt curve from 65 °C to 95 °C at increments of 0.5 °C/0.5 s. Samples were evaluated in triplicate and data are representative of three independent experiments. The levels of mRNA were normalized to β-actin mRNA and presented as average $2^{-\Delta CT}$ $[\Delta C_T = C_{T\ (gene\ of\ interest)} - C_{T\ (\beta\text{-}actin)}]$ expression values.

Declarations of interest

None.

Acknowledgements

We thank Dr. Xufang Deng, Matthew Hackbart, Aaron Volk, Dr. Michael Hantak, Enya Qing, Nicole André and Javier Jaimes for helpful discussions. We also thank Drs. Fred Scott, Edward J. Dubovi, Thomas Gallagher and Edward Campbell for the provision of reagents. This work was supported by a Pilot Project grant issued to S.C.B. by Loyola University of Chicago and a research grant from the Winn Feline Foundation Bria Fund (MTW17-022 to S.C.B. and G.R.W.). R.C.M. was supported by the National Institutes of Health (NIH) R01 AI085089 (to S.C.B.), NIH T32 Training Grant for Experimental Immunology (AI007508), and the Arthur J. Schmitt Dissertation Fellowship in Leadership and Service (Arthur J. Schmitt Foundation). G.R.W. is supported by research grants from the Cornell Feline Health Center and the Winn Feline Foundation.

References

Addie, D.D., 2011. Feline coronaviral infections. In: Greene, C. (Ed.), Infectious Diseases of the Dog and Cat. Saunders, pp. 92–108.

Addie, D.D., Jarrett, O., 1992. A study of naturally occurring feline coronavirus infections in kittens. Vet. Rec. 130, 133–137. https://doi.org/10.1136/vr.130.7.133.

Addie, D.D., Schaap, I.A.T., Nicolson, L., Jarrett, O., 2003. Persistence and transmission of natural type I feline coronavirus infection. J. Gen. Virol. 84, 2735–2744. https://doi.org/10.1099/vir.0.19129-0.

Belouzard, S., Millet, J.K., Licitra, B.N., Whittaker, G.R., 2012. Mechanisms of coronavirus cell entry mediated by the viral spike protein. Viruses 4, 1011–1033. https://doi.org/10.3390/v4061011.

Bertram, S., Dijkman, R., Habjan, M., Heurich, A., Gierer, S., Glowacka, I., Welsch, K., Winkler, M., Schneider, H., Hofmann-Winkler, H., Thiel, V., Pohlmann, S., 2013. TMPRSS2 activates the human coronavirus 229E for cathepsin-independent host cell entry and is expressed in viral target cells in the respiratory epithelium. J. Virol. 87, 6150–6160. https://doi.org/10.1128/jvi.03372-12.

Channappanavar, R., Fehr, A.R., Vijay, R., Mack, M., Zhao, J., Meyerholz, D.K., Perlman, S., 2016. Dysregulated type I interferon and inflammatory monocyte-macrophage responses cause lethal pneumonia in SARS-CoV-infected mice. Cell Host Microbe 19, 181–193. https://doi.org/10.1016/j.chom.2016.01.007.

Corapi, W.V., Olsen, C.W., Scott, F.W., 1992. Monoclonal antibody analysis of neutralization and antibody-dependent enhancement of feline infectious peritonitis virus. J. Virol. 66, 6695–6705.

de Groot-Mijnes, J.D.F., van Dun, J.M., van der Most, R.G., de Groot, R.J., 2004. Natural history of a recurrent feline coronavirus infection and the role of cellular immunity in survival and disease. J. Virol. 79, 1036–1044. https://doi.org/10.1128/jvi.79.2.1036-1044.2005.

de Haan, C.A.M., Haijema, B.J., Schellen, P., Schreur, P.W., Te Lintelo, E., Vennema, H., Rottier, P.J.M., 2008. Cleavage of group 1 coronavirus spike proteins: how furin cleavage is traded off against heparan sulfate binding upon cell culture adaptation. J. Virol. 82, 6078–6083. https://doi.org/10.1128/JVI.00074-08.

Dedeurwaerder, A., Desmarets, L.M., Olyslaegers, D.A.J., Vermeulen, B.L., Dewerchin, H.L., Nauwynck, H.J., 2013. The role of accessory proteins in the replication of feline infectious peritonitis virus in peripheral blood monocytes. Vet. Microbiol. 162, 447–455. https://doi.org/10.1016/j.vetmic.2012.10.032.

Dedeurwaerder, A., Olyslaegers, D.A.J., Desmarets, L.M.B., Roukaerts, I.D.M., Theuns, S., Nauwynck, H.J., 2014. ORF7-encoded accessory protein 7a of feline infectious peritonitis virus as a counteragent against IFN-α-induced antiviral response. J. Gen. Virol. 95, 393–402. https://doi.org/10.1099/vir.0.058743-0.

Deng, X., Hackbart, M., Mettelman, R.C., O'Brien, A., Mielech, A.M., Yi, G., Kao, C.C., Baker, S.C., 2017. Coronavirus nonstructural protein 15 mediates evasion of dsRNA sensors and limits apoptosis in macrophages. Proc. Natl. Acad. Sci. 114, E4251–E4260. https://doi.org/10.1073/pnas.1618310114.

Deng, X., van Geelen, A., Buckley, A.C., O'Brien, A., Pillatzki, A., Lager, K.M., Faaberg, K.S., Baker, S.C., 2019. Coronavirus endoribonuclease activity in porcine epidemic diarrhea virus suppresses type I and type III interferon responses. J. Virol. 93, e02000–18. https://doi.org/10.1128/JVI.02000-18.

Du, Y., Xin, L., Shi, Y., Zhang, T.H., Wu, N.C., Dai, L., Gong, D., Brar, G., Shu, S., Luo, J., Reiley, W., Tseng, Y.W., Bai, H., Wu, T.T., Wang, J., Shu, Y., Sun, R., 2018. Genome-wide identification of interferon-sensitive mutations enables influenza vaccine design. Science 359, 290–296. https://doi.org/10.1126/science.aan8806.

Earnest, J.T., Hantak, M.P., Li, K., McCray, P.B., Perlman, S., Gallagher, T., 2017. The tetraspanin CD9 facilitates MERS-coronavirus entry by scaffolding host cell receptors and proteases. PLoS Pathog. 13, e1006546. https://doi.org/10.1371/journal.ppat.1006546.

Fensterl, V., Sen, G.C., 2011. The ISG56/IFIT1 gene family. J. Interferon Cytokine Res. 31, 71–78. https://doi.org/10.1089/jir.2010.0101.

Glowacka, I., Bertram, S., Muller, M.A., Allen, P., Soilleux, E., Pfefferle, S., Steffen, I., Tsegaye, T.S., He, Y., Gnirss, K., Niemeyer, D., Schneider, H., Drosten, C., Pohlmann, S., 2011. Evidence that TMPRSS2 activates the Severe Acute Respiratory Syndrome Coronavirus spike protein for membrane fusion and reduces viral control by the humoral immune response. J. Virol. 85, 4122–4134. https://doi.org/10.1128/JVI.02232-10.

Hoebe, K., Janssen, E., Beutler, B., 2004. The interface between innate and adaptive immunity. Nat. Immunol. 5, 971–974. https://doi.org/10.1038/ni1004-971.

Hohdatsu, T., Izumiya, Y., Yokoyama, Y., Kida, K., Koyama, H., 1998. Differences in virus receptor for type I and type II feline infectious peritonitis virus. Arch. Virol. 143, 839–850. https://doi.org/10.1007/s007050050336.

Hohdatsu, T., Okada, S., Ishizuka, Y., Yamada, H., Koyama, H., 1992. The prevalence of types I and II feline coronavirus infections in cats. J. Vet. Med. Sci. 54, 557–562. https://doi.org/10.1292/jvms.54.557.

Hohdatsu, T., Okada, S., Koyama, H., 1991. Characterization of monoclonal antibodies against feline infectious peritonitis virus type II and antigenic relationship between feline, porcine, and canine coronaviruses. Arch. Virol. 117, 85–95. https://doi.org/10.1007/BF01310494.

Huber, J.P., David Farrar, J., 2011. Regulation of effector and memory T-cell functions by type I interferon. Immunology 132, 466–474. https://doi.org/10.1111/j.1365-2567.2011.03412.x.

Kessler, Y., Helfer-Hungerbuehler, A.K., Cattori, V., Meli, M.L., Zellweger, B., Ossent, P., Riond, B., Reusch, C.E., Lutz, H., Hofmann-Lehmann, R., 2009. Quantitative TaqMan®real-time PCR assays for gene expression normalisation in feline tissues. BMC Mol. Biol. 10, 106. https://doi.org/10.1186/1471-2199-10-106.

Kim, Y., Liu, H., Galasiti Kankanamalage, A.C., Weerasekara, S., Hua, D.H., Groutas, W.C., Chang, K.O., Pedersen, N.C., 2016. Reversal of the progression of fatal coronavirus infection in cats by a broad-spectrum coronavirus protease inhibitor. PLoS Pathog. 12, e1005531. https://doi.org/10.1371/journal.ppat.1005531.

Kim, Y., Lovell, S., Tiew, K.-C., Mandadapu, S.R., Alliston, K.R., Battaile, K.P., Groutas, W.C., Chang, K.-O., 2012. Broad-spectrum antivirals against 3C or 3C-like proteases of picornaviruses, noroviruses, and coronaviruses. J. Virol. 86, 11754–11762. https://doi.org/10.1128/JVI.01348-12.

Kim, Y., Mandadapu, S., Groutas, W., Chang, K., 2013. Potent inhibition of feline coronaviruses with peptidyl compounds targeting coronavirus 3C-like protease. Antivir. Res. 97, 161–168. https://doi.org/10.1016/j.antiviral.2012.11.005.Potent.

Kim, Y., Shivanna, V., Narayanan, S., Prior, A.M., Weerasekara, S., Hua, D.H., Kankanamalage, A.C., Groutas, W.C., Chang, K.O., 2015. Broad-spectrum inhibitors against 3C-like proteases of feline coronaviruses and feline caliciviruses. J. Virol. 89, 4942–4950. https://doi.org/10.1128/JVI.03688-14.

Kindler, E., Gil-Cruz, C., Spanier, J., Li, Y., Wilhelm, J., Rabouw, H.H., Züst, R., Hwang, M., V'kovski, P., Stalder, H., Marti, S., Habjan, M., Cervantes-Barragan, L., Elliot, R., Karl, N., Gaughan, C., van Kuppeveld, F.J.M., Silverman, R.H., Keller, M., Ludewig, B., Bergmann, C.C., Ziebuhr, J., Weiss, S.R., Kalinke, U., Thiel, V., 2017. Early endonuclease-mediated evasion of RNA sensing ensures efficient coronavirus replication. PLoS Pathog. 13, e1006195. https://doi.org/10.1371/journal.ppat.1006195.

Kipar, A., Meli, M.L., 2014. Feline infectious peritonitis: still an enigma? Vet. Pathol. 51, 505–526. https://doi.org/10.1177/0300985814522077.

Krenke, B.E., Ekenberg, S., Frackman, S., Hoffmann, K., Sprecher, C.J., Storts, D.R., 2005. Development of a novel , fluorescent , two-primer approach to quantitative PCR. Promega Profiles DNA 3–5.

Licitra, B.N., Millet, J.K., Regan, A.D., Hamilton, B.S., Rinaldi, V.D., Duhamel, G.E., Whittaker, G.R., 2013. Mutation in spike protein cleavage site and pathogenesis of feline coronavirus. Emerg. Infect. Dis. 19, 1066–1073. https://doi.org/10.3201/eid1907.121094.

Meager, A., 2006. The Interferons : Characterization and Application. Wiley-VCH.

Menachery, V.D., Gralinski, L.E., Mitchell, H.D., Dinnon, K.H., Leist, S.R., Yount, B.L., McAnarney, E.T., Graham, R.L., Waters, K.M., Baric, R.S., 2018. Combination attenuation offers strategy for live attenuated coronavirus vaccines. J. Virol. 92 e00710-18. https://doi.org/10.1128/jvi.00710-18.

Merck Veterinary Manual, 2015. Gastric dilation and volvulus in small animals: diseases of the stomach and intestines in small animals. [WWW Document]. http://www.merckvetmanual.com accessed 7.1.18.

Millet, J.K., Whittaker, G.R., 2015. Host cell proteases: critical determinants of coronavirus tropism and pathogenesis. Virus Res. 202, 120–134. https://doi.org/10.1016/j.virusres.2014.11.021.

O'Brien, A., Mettelman, R.C., Volk, A., André, N.M., Whittaker, G.R., Baker, S.C., 2018. Characterizing replication kinetics and plaque production of type I feline infectious peritonitis virus in three feline cell lines. Virology 525, 1–9. https://doi.org/10.

1016/J.VIROL.2018.08.022.
Olsen, C.W., Corapi, W.V., Ngichabe, C.K., Baines, J.D., Scott, F.W., 1992. Monoclonal antibodies to the spike protein of feline infectious peritonitis virus mediate antibody-dependent enhancement of infection of feline macrophages. J. Virol. 66, 956–965.
Park, J.-E., Li, K., Barlan, A., Fehr, A.R., Perlman, S., McCray, P.B., Gallagher, T., 2016. Proteolytic processing of Middle East respiratory syndrome coronavirus spikes expands virus tropism. Proc. Natl. Acad. Sci. 113, 12262–12267. https://doi.org/10.1073/pnas.1608147113.
Pedersen, N.C., 2014a. An update on feline infectious peritonitis: diagnostics and therapeutics. Vet. J. 201, 133–141. https://doi.org/10.1016/j.tvjl.2014.04.016.
Pedersen, N.C., 2014b. An update on feline infectious peritonitis: virology and immunopathogenesis. Vet. J. 201, 123–132. https://doi.org/10.1016/j.tvjl.2014.04.017.
Pedersen, N.C., 2009. A review of feline infectious peritonitis virus infection: 1963-2008. J. Feline Med. Surg. 11, 225–258. https://doi.org/10.1016/j.jfms.2008.09.008.
Pedersen, N.C., Black, J.W., Boyle, J.F., Evermann, J.F., McKeirnan, A.J., Ott, R.L., 1984. Pathogenic differences between various feline coronavirus isolates. In: Molecular Biology and Pathogenesis of Coronaviruses. Springer, Boston, MA, pp. 365–380. https://doi.org/10.1007/978-1-4615-9373-7_36.
Pedersen, N.C., Kim, Y., Liu, H., Galasiti Kankanamalage, A.C., Eckstrand, C., Groutas, W.C., Bannasch, M., Meadows, J.M., Chang, K.O., 2018. Efficacy of a 3C-like protease inhibitor in treating various forms of acquired feline infectious peritonitis. J. Feline Med. Surg. 20, 378–392. https://doi.org/10.1177/1098612X17729626.
Pedersen, N.C., Perron, M., Bannasch, M., Montgomery, E., Murakami, E., Liepnieks, M., Liu, H., 2019. Efficacy and safety of the nucleoside analog GS-441524 for treatment of cats with naturally occurring feline infectious peritonitis. J. Feline Med. Surg. 21, 271–281. https://doi.org/10.1177/1098612X19825701.
Reinke, L.M., Spiegel, M., Plegge, T., Hartleib, A., Nehlmeier, I., Gierer, S., Hoffmann, M., Hofmann-Winkler, H., Winkler, M., Pöhlmann, S., 2017. Different residues in the SARS-CoV spike protein determine cleavage and activation by the host cell protease TMPRSS2. PLoS One 12, e0179177. https://doi.org/10.1371/journal.pone.0179177.
Rose, K.M., Weiss, S.R., 2009. Murine coronavirus cell type dependent interaction with the type I interferon response. Viruses 1, 689–712. https://doi.org/10.3390/v1030689.
Satoh, R., Kaku, A., Satomura, M., Kohori, M., Noura, K., Furukawa, T., Kotake, M., Takano, T., Hohdatsu, T., 2011. Development of monoclonal antibodies (MAbs) to feline interferon (fIFN)-γ as tools to evaluate cellular immune responses to feline infectious peritonitis virus (FIPV). J. Feline Med. Surg. 13, 427–435. https://doi.org/10.1016/J.JFMS.2011.01.008.
Shalem, O., Sanjana, N.E., Hartenian, E., Shi, X., Scott, D.A., Mikkelsen, T.S., Heckl, D., Ebert, B.L., Root, D.E., Doench, J.G., Zhang, F., 2014. Genome-scale CRISPR-Cas9 knockout screening in human cells. Science (80-) 343, 84–87. https://doi.org/10.1126/science.1247005.
Shirato, K., Kanou, K., Kawase, M., Matsuyama, S., 2016. Clinical isolates of human coronavirus 229E bypass the endosome for cell entry. J. Virol. 91 e01387-16. https://doi.org/10.1128/jvi.01387-16.
Shirato, K., Kawase, M., Matsuyama, S., 2013. Middle East Respiratory Syndrome Coronavirus infection mediated by the transmembrane serine protease TMPRSS2. J. Virol. 87, 12552–12561. https://doi.org/10.1128/jvi.01890-13.
Siegrist, C.-A., 2013. In: Plotkin, S.A., Orenstein, W.A., Offit, P.A. (Eds.), Vaccine Immunology. Vaccines Elsevier Inc., pp. 14–32. https://doi.org/10.1016/B978-1-4557-0090-5.00004-5.
St John, S.E., Therkelsen, M.D., Nyalapatla, P.R., Osswald, H.L., Ghosh, A.K., Mesecar, A.D., St John, S.E., Therkelsen, M.D., Nyalapatla, P.R., Osswald, H.L., Ghosh, A.K., Mesecar, A.D., 2015. X-ray structure and inhibition of the feline infectious peritonitis virus 3C-like protease: structural implications for drug design. Bioorg. Med. Chem. Lett 25, 5072–5077. https://doi.org/10.1016/j.bmcl.2015.10.023.
Tang, F., Quan, Y., Xin, Z.-T., Wrammert, J., Ma, M.-J., Lv, H., Wang, T.-B., Yang, H., Richardus, J.H., Liu, W., Cao, W.-C., 2011. Lack of peripheral memory B cell responses in recovered patients with severe acute respiratory syndrome: a six-year follow-up study. J. Immunol. 186, 7264–7268. https://doi.org/10.4049/jimmunol.0903490.
Tekes, G., Spies, D., Bank-Wolf, B., Thiel, V., Thiel, H.-J.H.-J., 2012. A reverse genetics approach to study feline infectious peritonitis. J. Virol. 86, 6994–6998. https://doi.org/10.1128/JVI.00023-12.
Thiel, V., Thiel, H.-J., Tekes, G., 2014. Tackling feline infectious peritonitis via reverse genetics. Bioengineered 5, 396–400. https://doi.org/10.4161/bioe.32133.
Totura, A.L., Baric, R.S., 2012. SARS coronavirus pathogenesis: host innate immune responses and viral antagonism of interferon. Curr. Opin. Virol. 2, 264–275. https://doi.org/10.1016/j.coviro.2012.04.004.
Tough, D.F., 2012. Modulation of T-cell function by type I interferon. Immunol. Cell Biol. 90, 492–497. https://doi.org/10.1038/icb.2012.7.
Vennema, H., Poland, A., Foley, J., Pedersen, N.C., 1998. Feline infectious peritonitis viruses arise by mutation from endemic feline enteric coronaviruses. Virology 243, 150–157. https://doi.org/10.1006/viro.1998.9045.
Whittaker, G.R., André, N.M., Millet, J.K., 2018. Improving virus taxonomy by re-contextualizing sequence-based classification with biologically relevant data: the case of the Alphacoronavirus 1 species. mSphere 3, e00413–e00417. https://doi.org/10.1128/mSphere.00463-17.